



Biogenic Synthesis and Characterization of Silver Nanoparticles Using a Combined Leaf Extract for Anti-Bacterial and Biofilm Inhibition Properties

Mathan Chandrasekaran, Uma Chinnaiyan, Sowndarya Sivaprakasam, Sivagurunathan Paramasivam*

*Department of Microbiology, Faculty of Science, Annamalai University, Chidambaram – 608002, Tamil Nadu, India***ARTICLE INFO***Article history:*

Received 29 January 2025

Revised 06 February 2025

Accepted 15 February 2025

Published online 01 April 2025

ABSTRACT

The environmentally friendly production of silver nanoparticles (AgNPs) involves using plant material to develop biocompatible antibacterial substances, presenting sustainable substitutes for harmful chemicals. This study aimed to optimize the green synthesis of AgNPs utilizing leaf extracts from *Raphanus sativus*, *Ipomoea batatas*, and *Ananas comosus*. Various characterization techniques employed for the synthesized nanoparticles included UV-Visible spectrophotometry, FTIR (Fourier Transform Infrared) spectrophotometry, XRD (X-ray Diffraction), SEM (Scanning Electron Microscopy), TEM (Transmission Electron Microscopy), and DLS (Dynamic Light Scattering). The antibacterial and antibiofilm properties of nanoparticles were screened. A noticeable color change confirmed the formation of nanoparticles. The UV-visible spectrophotometer displayed an absorbance peak at 450 nm. FTIR analysis identified the compounds that facilitated the reduction of silver ions, with functional groups such as OH, C-H, CHO, and N-H being detected. The DLS analysis indicated a zeta potential of -25.1 mV and a zeta average size of 62.44 d.nm. SEM examination revealed the silver nanoparticles as rod-shaped, measuring between 73.13 and 84.85 nm, while TEM showed spherical morphologies with an approximate size of 5 nm. The silver nanoparticles exhibited antibacterial properties against four gram-negative bacteria. Among them, AgNPs yield the highest zone of inhibition against *Pseudomonas aeruginosa*. The biofilm inhibitory capabilities of the biologically synthesized silver nanoparticles were assessed using Congo Red Agar, which provided qualitative results, and the microtiter plate method, which supplied quantitative data against *Pseudomonas aeruginosa*, a planktonic organism. This study highlights the potential applications of silver nanoparticles in addressing microbial kinetics, underlining their antibacterial and anti-biofilm effectiveness.

Copyright: © 2025 Chandrasekaran *et al.* This is an open-access article distributed under the terms of the [Creative Commons Attribution License](https://creativecommons.org/licenses/by/4.0/), which permits unrestricted use, distribution, and reproduction in any medium, provided the original author and source are credited.

Keywords: *Raphanus sativus*, *Ananas comosus*, *Ipomoea batatas*, Silver nanoparticles, *Pseudomonas aeruginosa*.

Introduction

Nanotechnology innovations offer sustainable and environmentally benign methods to convert leaf waste into nanoparticles, adhering to green chemistry principles. This process utilizes the bioactive compounds of the leaves as reducing agents and stabilizers, which is preferable to traditional chemical synthesis, which often involves hazardous substances and high energy consumption.¹ Transforming leaf waste into nanoparticles will result in size ranges between 1 and 100 nm with unique properties representing a significant advancement in sustainable nanotechnology.² Recent progress in green synthesis using natural agents has focused on biological methods as NPs are widely utilized in human-exposed environments. Although physicochemical methods can produce NPs, they are resource-intensive and involve toxic solvents, hazardous by-products, and surface imperfections.³ Natural extracts serve as an eco-friendly alternative to expensive chemical reducing agents in the green synthesis of metal or metal oxide nanoparticles (NPs).

This bottom-up approach offers a biogenic method for reducing metal precursors to NPs, which is not only environmentally sustainable and chemical-free but also cost-effective and scalable for industrial applications.¹ Plant extracts are frequently selected for NP production because of their value and suitability for large-scale environmentally benign synthesis.² Although the green synthesized AgNPs have been extensively investigated, research on the biosynthesis and applications of other metal and semiconductor NPs remains limited. Biofilm formation is crucial in antibiotic resistance, as these microbial structures adhere to surfaces and are encased in extracellular polymeric substances (EPS). This process begins with planktonic bacteria attaching to a surface. The presence of biofilms significantly enhances bacterial resistance to antimicrobial agents, including antibiotics. The increased resistance is linked to the extracellular polymeric substance (EPS) matrix, which hinders the entry of these agents. As a result, higher concentrations are required to achieve effective outcomes.⁴ The rise in multidrug-resistant infections has prompted the exploration of alternatives, such as silver nanoparticles, known for their strong bactericidal properties.⁵ AgNPs primarily act by releasing Ag⁺ ions, which disrupt bacterial cell membranes and essential processes leading to cell death.⁶ Nonetheless, existing research has largely emphasized the effectiveness of AgNPs in addressing bacteria that are linked to biofilm formation.

Raphanus sativus, a popular vegetable, has been used in medicinal practices for cardiovascular, liver, gastrointestinal, and infections. Producing silver nanoparticles from radish leaves are more environmentally friendly method and on the other hand, they are not typically consumed by humans.⁷ They present promising avenues for further investigation, potentially serving as anticancer agents. *Ipomoea batatas*, the sixth most abundant food crop globally, is rich in antioxidant properties and medicinal applications.⁸

*Corresponding author. Email: sivaguru1981@gmail.com
Tel: 9940769774

Citation: Chandrasekaran M, Chinnaiyan U, Sivaprakasam S, Paramasivam S. Biogenic Synthesis and Characterisation of Silver Nanoparticles Using a Combined Leaf Extract for Anti-Bacterial and Biofilm Inhibition Properties. Trop J Nat Prod Res. 2025; 9(3): 1089 – 1096 <https://doi.org/10.26538/tjnpr/v9i3.25>

Official Journal of Natural Product Research Group, Faculty of Pharmacy, University of Benin, Benin City, Nigeria

Various antioxidant compounds, including phenolic compounds, flavonoids, beta-carotene, anthocyanins, and caffeoylquinic acid derivatives, have been employed in traditional medicinal practices to remedy oral health problems.⁹ A novel and environmentally friendly method for synthesizing silver nanoparticles has been suggested, utilizing sweet potato leaf extract as a potential agent for both reduction and capping processes.¹⁰

Research in Taiwan has revealed promising results in the synthesis of silver nanoparticles using agricultural byproducts, specifically *Ananas comosus* leaves. The phytochemicals found in these leaves function as both reducing and capping agents, facilitating the creation of stable oligomeric silver nanoparticle clusters. This innovative approach to nanoparticle production could have significant implications for biomedical applications.¹¹

While research on the bioactivity of silver nanoparticles synthesised from combined three leaves extract is extensive, there remains a significant gap, particularly in its role as an antibacterial and antibiofilm agent against *Escherichia coli*, *Klebsiella aerogenes*, *Acinetobacter baumannii*, and *Pseudomonas aeruginosa*. The research aims to explore the antimicrobial properties of silver nanoparticles (AgNPs) derived from above three distinct leaf varieties, with a particular emphasis on their capacity to suppress the development of biofilms.

Materials and Methods

Collection of leaves

Leaves of *Raphanus sativus* (10°55'44.8"N, 79°23'35.3"E), *Ipomoea batatas* (10°55'40.4"N, 79°24'10.6"E), and *Ananas comosus* (10°55'53.3"N, 79°23'41.4"E) were collected in and around Korukai, Thanjavur District, Tamil Nadu, on December 2021.

Preparation of Aqueous extract

To prepare the aqueous extracts, leaf samples were initially subjected to thorough cleansing to eliminate impurities and fungal spores, followed by desiccation to remove moisture. The three leaf varieties were subsequently pulverized into fine powder using an electric grinder. A 250 mL beaker was used to combine 200 ml of distilled water with a 10 g leaf mixture, which consisted of 3.3 g each from three different leaf types. The solution was subsequently subjected to heating in a mantle for 45 minutes. Following this, the extracts were permitted to cool at room temperature before undergoing filtration. This procedure is consistently applied to the preparation of all plant extracts in this study.¹²

AgNPs synthesis

The synthesis of AgNPs was carried out by mixing AgNO₃ solution with water extract of the leaves of three plants. The optimal concentration of AgNO₃ solution at 2.0mM was determined for subsequent nanoparticle synthesis. Determination of the optimal concentration of AgNO₃ was carried out by adding 90 ml of aqueous solution of AgNO₃ (2 mM) with 10 mL of aqueous extract of *Raphanus sativus*, *Ipomoea batatas*, and *Ananas comosus* which is placed in a shaker incubator which rotated constantly for 8 hours at room temperature. Colour change to dark brown was taken as an indication of synthesis of AgNPs. Then, the maximum absorption wavelength was determined using a UV-Vis spectrophotometer.¹³

Investigated microorganisms for antimicrobial activity

A study was undertaken to evaluate the antimicrobial properties of silver nanoparticles against four Gram-negative bacterial species: *Escherichia coli*, *Klebsiella aerogenes*, *Pseudomonas aeruginosa*, and *Acinetobacter baumannii*. The bacterial cultures were maintained on a nutrient agar medium composed of peptone, beef extract, and sodium chloride. To prepare for the experiments, the strains were initially grown in nutrient broth, promoting microbial proliferation during the logarithmic growth phase.

Characterization of synthesized Ag NPs

Fourier transform infrared study

Functional group identification in the AgNPs was conducted using Fourier-transform infrared (FTIR) spectroscopy (Bruker Alpha T, Germany). This analytical technique provides insights into the molecular structure, typically derived from absorption spectra. To prepare a 50 ml AgNP colloid solution for FTIR analysis, optimal conditions were employed, including EFE (5%), 1 mM silver nitrate, and centrifugation at 20,000 rpm for 20 min. The pellets obtained were re-suspended and then lyophilized for a period of 16 hours.¹⁴ This analytical technique provides insights into the molecular structure, typically derived from absorption spectra.

UV-Visible spectrophotometry

The bio-reduction of silver ions in solution was monitored using UV-visible absorption spectroscopy. A UV-visible spectrophotometer was employed to capture the spectra of the produced AgNPs. The absorption spectra were documented using a Shimadzu Co. UV-1800 spectrophotometer (Japan), scanning from 200 to 800 nm with 1 nm resolution. AgNPs emit light at wavelengths ranging from 400 to 800 nm, depending on their size, structure, and arrangement.¹⁵

X-ray diffraction (XRD)

For the X-ray diffraction (XRD) analysis, researchers applied the AgNP solution to a glass microscope slide. Desiccation of the samples took place in a heated air oven (HAO) set to 50 °C. This step was repeated until a uniform single layer was achieved. Analysis of the dried sample was then conducted using an X-ray diffractometer, Pan Analytical X-pert pro system, Netherlands. This equipment utilizes a copper (Cu) source and operates with a voltage of 45 kV and a current of 40 mA.¹⁶

Scanning electron microscope (SEM)

Scanning electron microscopy (SEM) was used for analyzing the shape and form of AgNPs. The nanoparticles were processed by means of centrifugation at 15,000 rpm for 10 min. After which, the pellets were collected and further dried in a dehydration oven (50 °C) to remove residual moisture. The dried powder of silver nanoparticles obtained from the above method was subjected to energy-dispersive X-ray diffraction (XRD) using a Bruker X-flash finder (Bruker, Bremen, Germany). The prepared samples were investigated using an FEI Nova Nanolab 200 SEM (FEI Company Hillsboro, OR, USA). For all imaging and energy-dispersive X-ray (EDX) analyses the energy of the electron beam was set to 15 keV.¹⁷

Transmission electron microscope (TEM)

Transmission electron microscopy (Philips Tecnai G-10, Netherlands) was utilized to analyze the morphological characteristics of the synthesized nanoparticles (NPs). The process involved applying a single drop of the sample onto a copper grid, which was then dried under vacuum conditions. Images of the dried nanoemulsion were captured by TEM apparatus operates at 80 kV and is equipped with a tungsten source and an ultrahigh-resolution pole piece, achieving a resolution of 1.9 Å.¹⁸

Dynamic Light Scattering (DLS)

A portion of the synthesized nanoparticles was transferred into a plastic cuvette, and their average particle size and polydispersity index (PDI) were measured using dynamic light scattering (DLS) at 25°C with a detection angle of 90° via photon correlation spectroscopy (PCS). The nanoparticle dispersions were diluted with redistilled water to optimize the signal strength for the instrument, depending on the drug concentration. The zeta potential of the nanoparticles was analyzed using a Malvern Zetasizer Nano series (Malvern Instruments Ltd., Malvern, UK).¹⁹

Antimicrobial assay

Well diffusion technique

To analyze the antimicrobial effect of the produced Ag NPs, the agar-based well diffusion technique was utilized. Twenty milliliters of semi-solid Mueller-Hinton agar (MHA) medium were used to prepare Petri dishes. Four test bacteria (*Klebsiella aerogenes*, *Pseudomonas*

aeruginosa, *Escherichia coli*, and *Acanitobacter baumannii*) were grown in nutrient broth for 24 hours.

Following this, suspensions containing 1.5×10^8 CFU/mL were distributed on the MHA surface using a sterile brush. Six-millimeter diameter wells were then created in the inoculated plates and filled with AgNPs at concentrations from 25 to 100 $\mu\text{g/mL}$. The plates containing the four bacterial species were incubated for 24 hours at 37°C. In the experiment, tetracycline was utilized as a positive control. The effectiveness of the antimicrobial agent was evaluated by determining the size of the inhibition zone, which was measured in millimeters.²⁰

Minimum Inhibitory Concentration (MIC)

The Minimum Inhibitory Concentration (MIC) is the least concentration that suppresses maximal microbial proliferation. This methodology involves the cultivation of microorganisms in suspensions containing various concentrations of silver nanoparticles. The experimental procedure was initiated by allocating 5 ml of nutrient broth into five sterilized test tubes. Subsequently, distinct AgNP concentrations (10, 20, 30, 40, 50 $\mu\text{g/ml}$) were introduced into each tube, followed by the incorporation of 50 μl of fresh bacterial culture. Subsequently, the tubes were subjected to a 24-hour incubation at 37 °C. Data collection involved spectrophotometric measurements of optical density at 600 nm by (DROPLET, Digital Spectrophotometer, India). These measurements facilitated the construction of a graph illustrating the relationship between optical density and AgNP concentration. The concentration corresponding to the minimal optical density was designated as the MIC of AgNPs for a particular microorganism under examination.²¹

Anti-biofilm assay

Microtiter plate method

The anti-biofilm activity against *P. aeruginosa*, was evaluated using crystal violet assay. AgNPs concentrations of 50, 100, 150 and 200 $\mu\text{g/mL}$ were prepared using 96-well plate. Then 10 μL of bacterial suspension containing 1.5×10^8 CFU/mL (0.5 McFarland's standard) was inoculated into each well. Each test was performed in triplicate. After 24h incubation at 37°C, the growth medium was discarded, and the plates were washed with distilled water and stained with 200 μL of 0.4% crystal violet. After 20 min, the stain was removed, and the excess stain was rinsed off with tap water (three times, 200 μL , each) before adding 200 μL of 95% (v/v) ethanol

to solubilize the crystal violet. From the dissolved crystal violet into ethanol, 150 μL from each well were transferred to new 96 well plate for spectrophotometric measurement (OD590nm) in an ELISA reader.²²

Congo red method

A qualitative methodology for identifying biofilm-producing bacteria involves evaluating chromatic alterations of colonies cultivated on Congo Red Agar (CRA) media. Congo red, 0.8 g of Congo red, sucrose (36 g), and brain heart infusion agar (BHI) agar (37 g/L) were used to prepare the CRA medium. The experiment employed two Petri dishes: a control dish without silver nanoparticle (AgNP) treatment and another treated with AgNPs. Both dishes were inoculated with bacterial cultures. The colonies were evaluated for their ability to produce biofilms by observing morphological shifts after a 24-hour incubation at 37 °C. Additionally, this approach demonstrated that AgNPs directly hindered biofilm development.²³

Results and Discussion

Synthesis of AgNPs

AgNPs were synthesized using leaf extracts from *Raphanus sativus*, *Ipomoea batatas*, and *Ananas comosus*. When these aqueous extracts were introduced into the silver nitrate solution, a noticeable color transition occurred, progressing from a lighter to a darker shade of brown. This color shift serves as an indicator of AgNP formation, as illustrated in Figure 1. Similar observations regarding the brown color change as a sign of silver nanoparticle production were documented.²⁴

Characterization of AgNPs

UV-Visible spectra analysis

UV-Vis analysis confirmed the successful synthesis of AgNPs. The characteristic absorption peaks for AgNPs were detected between 410 and 800 nm, with the most prominent peak occurring at 450 nm (Figure 2). The results align with previously reported values, supporting the accuracy of the findings. Any variations may be attributed to differences in experimental conditions.²⁵ A similar study also identified a characteristic Ag peak at 420 nm, confirming the presence of silver nanoparticles. Variations in peak position or intensity may result from differences in synthesis conditions.²⁶

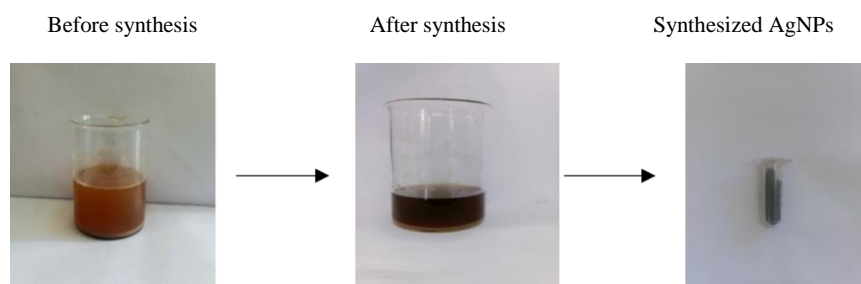


Figure 1: Synthesis of silver nanoparticle by using aqueous extracts of *Raphanus sativus*, *Ipomoea batatas* and *Ananas comosus* leaves.

FTIR (Fourier Transform Infra-Red spectroscopy)

FTIR (Fourier-transform infrared) spectroscopy is a key analytical technique that confirms the dual role of plant extracts as capping and reducing agents. Additionally, this method aids in identifying the essential functional groups that contribute significantly to the production of metal nanoparticles. To elucidate the biomolecules responsible for AgNP formation and stabilization, FTIR spectra were acquired using a Nicolet IS10 instrument, spanning the range of 400–4000 cm^{-1} . The spectra revealed that the synthesized AgNPs exhibited characteristic absorption peaks, with a band at 3470.40 cm^{-1} attributed to OH stretching, a band at 2832.10 cm^{-1} corresponding to aldehyde C-H stretching, and bands at 2719 cm^{-1} and 1630.30 cm^{-1} assigned to CHO and N-H, respectively, as depicted in Figure 3. FTIR spectroscopy

revealed functional groups in the leaf extract that were instrumental in both reducing and stabilizing silver nanoparticles (AgNPs). These constituents within the extract played a vital role in the formation process of AgNPs. These observations corroborate the occurrence of the reaction and successful formation of nanoparticles. A similar study demonstrated nanoparticle formation by detecting primary amine, carbonyl, and hydroxyl groups, along with other stabilizing functional moieties, using FTIR spectroscopy.²⁷

XRD (X-ray Diffraction)

The crystal structure of AgNPs was confirmed by X-ray diffraction analysis. Figure 4 displays the XRD patterns of AgNPs derived from *Raphanus sativus*, *Ipomoea batatas*, and *Ananas comosus* leaves. The

analysis revealed five characteristic diffraction peaks at 31.03°, 36.37°, 38.39°, 45.56°, and 65.60°, which were attributed to the 220, 200, 111,

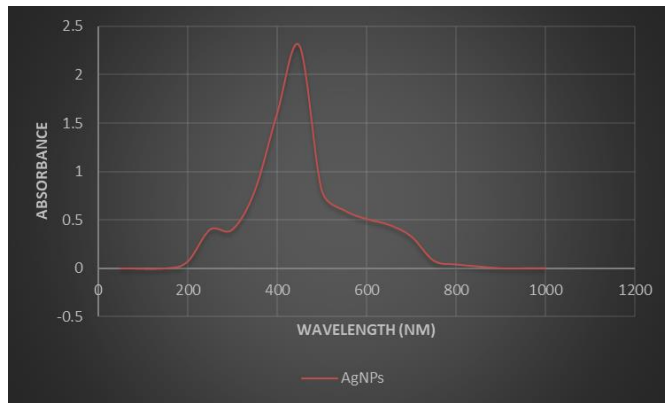


Figure 2: UV- visible spectrophotometry of synthesized AgNPs using *Raphanus sativus*, *Ipomoea batatas* and *Ananas comosus* leaves.

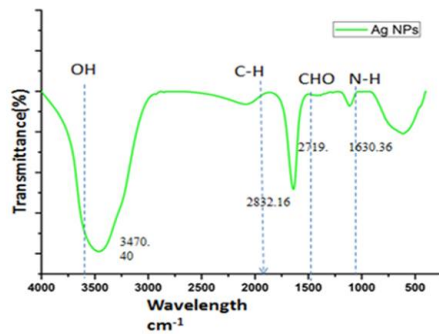


Figure 3: FTIR spectra of synthesized AgNPs from *Raphanus sativus*, *Ipomoea batatas* and *Ananas comosus* leaves.

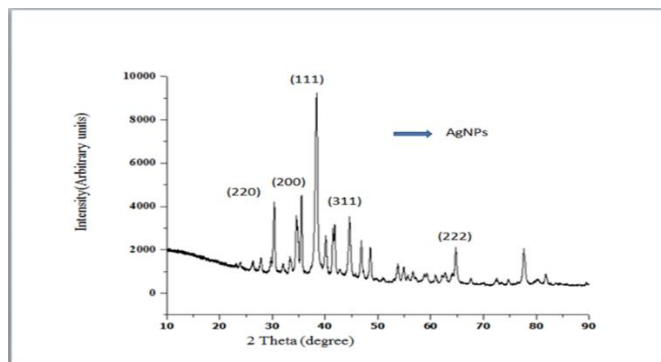


Figure 4 :X-ray diffraction analysis of biosynthesised AgNPs

311 and 222 crystallographic planes of silver, respectively. The diffraction peaks at 2θ values of 38.62°, 44.84°, 64.49°, and 77.32° are associated with the (111), (200), (220), and (311) crystal planes, respectively. These observations align with our findings and confirm the characteristic features of AgNPs, suggesting a face-centered cubic crystal structure.²⁸

SEM (Scanning Electron Microscope)

The precise structure of the AgNPs was revealed by SEM, which generally showed rod-shaped AgNPs in the Figure 5. The sizes ranged

from 73.13 to 84.85 nm at a magnification of 45k. A similar study reported smaller AgNP sizes, with both spherical and rod-like morphologies ranging from 6.13 nm to 32.04 nm and an average size of 15.76 nm. In contrast, the AgNPs obtained in this study ranged from 73.13 to 84.85 nm at a magnification of 45k, indicating a larger particle size.²⁴

Transmission Electron Microscope (TEM)

For preparation of TEM sample, the nanoparticles were diluted in water. Each TEM image shows uniformly dispersed nanoparticles. TEM analysis indicated that the synthesized AgNPs exhibited spherical morphology Figure 6. Based on the TEM images, the particles were estimated to be approximately 5 nm in size, with a considerable number predominantly exhibiting spherical shapes, as observed in a similar study.²⁹

Dynamic light scattering analysis (DLS)

The size and electrical charge of silver nanoparticles (AgNPs) synthesized using aqueous leaf extract from three combined leaves were examined through dynamic light scattering (DLS). Figures 7 (A & B) illustrate the DLS profile of these synthesized AgNPs. This technique was employed to assess the characteristics of the silver nanoparticles produced via the aqueous leaf extract from *Ananas comosus*, *Ipomoea batatas*, and *Raphanus sativus*. Metal nanoparticles (NPs) with a negative zeta potential exhibit an enhanced ability to traverse biological membranes and are less prone to aggregation or mutual adhesion.³⁰ A similar study reported silver nanoparticles synthesized using a microwave-assisted green synthesis method with an average particle size of approximately 98 nm and a zeta potential of -23.3 mV, as determined by dynamic light scattering (DLS) analysis. These findings align with our results, which also demonstrate AgNPs of similar size and surface charge characteristics.³¹

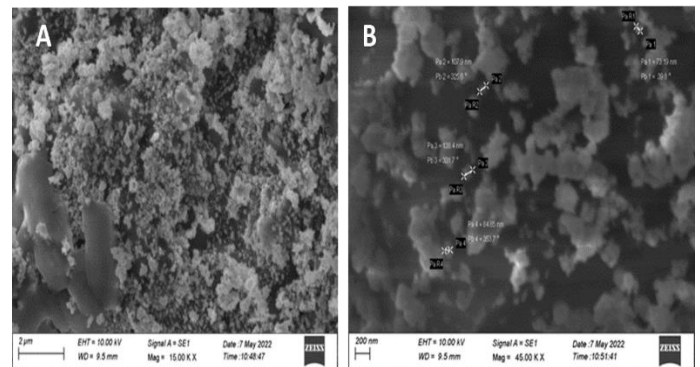


Figure 5: SEM images of the sample at (A) 15,000× magnification with a 2 µm scale bar, showing an aggregated morphology, and (B) 45,000× magnification with a 200 nm scale bar, highlighting individual nanoparticle sizes and distributions; both images were captured at 10.00 kV EHT using an SE1 detector.

The antimicrobial activity of biosynthesised AgNPs

Well diffusion technique.

The well diffusion technique, renowned for its efficiency and accuracy, was used to confirm the antimicrobial efficacy of AgNP extracted from three different leaf sources. The antibacterial potency of the AgNPs was assessed using various microbial strains, including *Escherichia coli*, *Klebsiella aerogenes*, *Acinetobacter baumannii*, and *Pseudomonas aeruginosa*. Silver nanoparticles derived from *Raphanus sativus*, *Ipomoea batatas*, and *Ananas comosus* were applied to the wells at varying concentrations (25, 50, 75, and 100 µg/ml). Tetracycline was used as the positive control (PC), while dimethyl sulfoxide (DMSO) was used as the negative control (NC). Figure 8 depict the antibacterial performance of AgNPs against bacterial cultures. *P.aeruginosa* demonstrated the most extensive inhibition zone when subjected to

AgNPs. The inhibition zone measurements obtained in this study align with findings from similar research, which examined both plant-derived

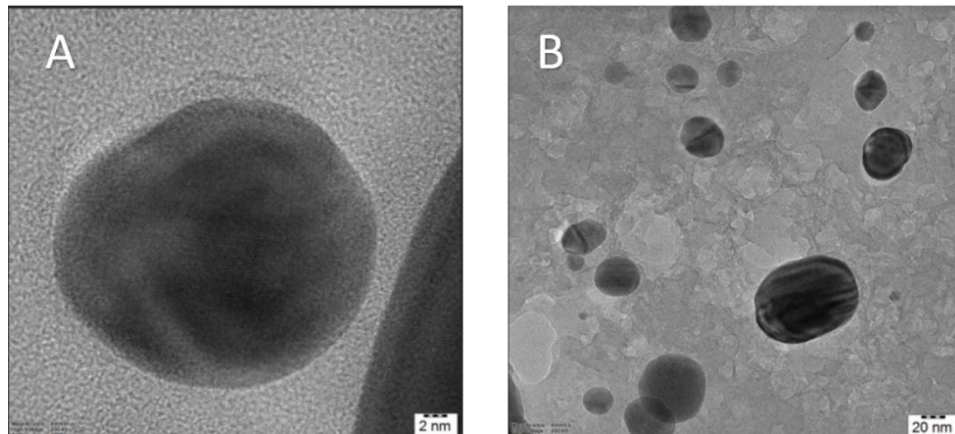


Figure 6: TEM images of the sample at (A) 300,000 \times magnification with a 2 nm scale bar, showing a single nanoparticle with high contrast, and (B) 200,000 \times magnification with a 20 nm scale bar, depicting multiple dispersed nanoparticles; both images were acquired at 300 kV accelerating voltage.

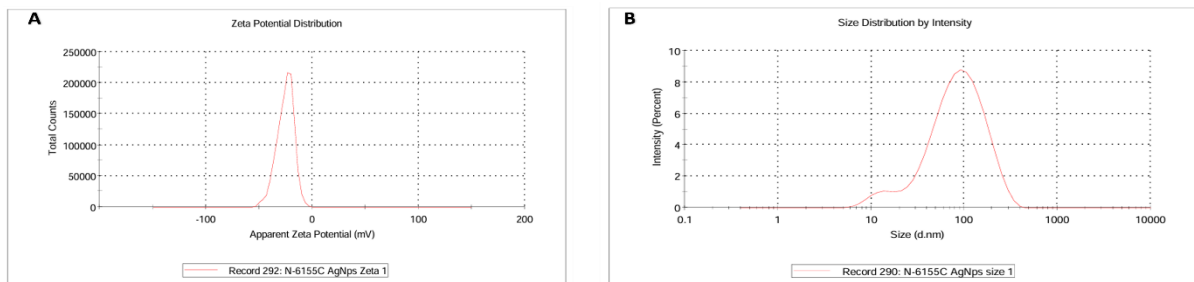


Figure 7: (A) The zeta potential and (B) size distribution value of the synthesized nanoparticles

and commercially synthesized silver nanoparticles and identified maximum inhibition zones at a concentration of 100 $\mu\text{g/ml}$.³²

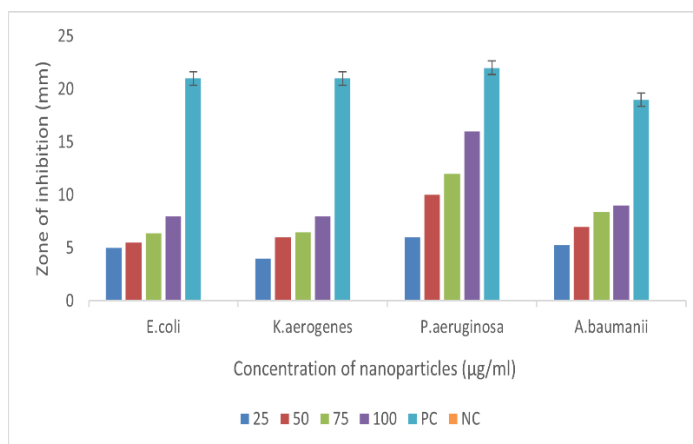


Figure 8: Zone of inhibition formed by various concentrations of biosynthesized silver nanoparticles

Minimal Inhibitory Concentration (MIC)

The biosynthesized AgNPs were analyzed to determine their MIC against *Pseudomonas aeruginosa*. The highest percentage of inhibition for AgNPs was observed at 50 $\mu\text{g/ml}$ concentration, corresponding to the minimum OD value of 0.02 nm, as illustrated in Figure 9. Figure 10 demonstrates that as the concentration of AgNPs increases, the broth's turbidity decreases, indicating greater inhibition of

Pseudomonas aeruginosa. A related study investigated the antibacterial activity of green-synthesized silver nanoparticles (AgNPs) against various Gram-negative foodborne pathogens. The minimum inhibitory concentration (MIC) values of the AgNPs ranged from 3.9 to 7.8 $\mu\text{g/ml}$, depending on the specific bacterial strain tested. These findings suggest that AgNPs exhibit potent antimicrobial properties against *Pseudomonas aeruginosa*.³³

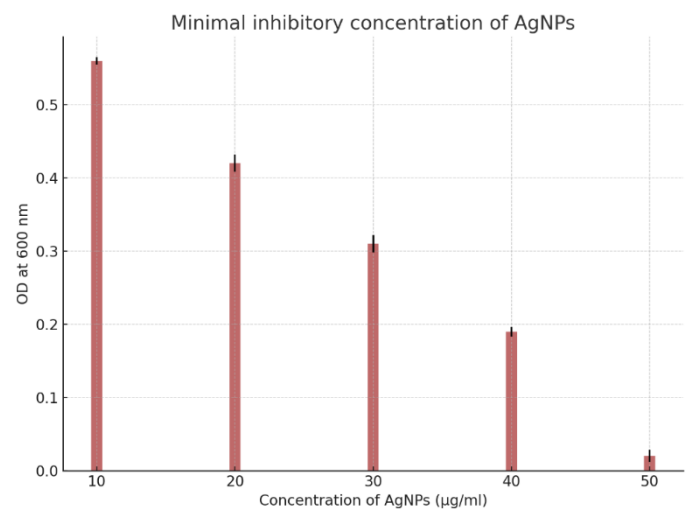


Figure 9: Minimal concentration of AgNPs for inhibition

Antibiofilm assay**Congo red assay**

Effect of AgNPs on biofilm inhibition on Congo Red Agar plates. The control Figure 11(A), demonstrating that the plate was not treated with AgNPs. Biofilm formation in the control plate indicated that *P.aeruginosa* was a biofilm-forming bacterium. Figure 11 (B) illustrates the plate treated with AgNPs and indicates biofilm inhibition. A similar study reported silver nanoparticles synthesized through a biosynthesis method, exhibiting effective inhibition of *Pseudomonas aeruginosa* biofilm formation as assessed by the Congo Red Agar assay. The results were consistent with our findings, where the biosynthesized AgNPs similarly disrupted biofilm formation and inhibited bacterial growth, suggesting their potential as effective antimicrobial agents.⁶

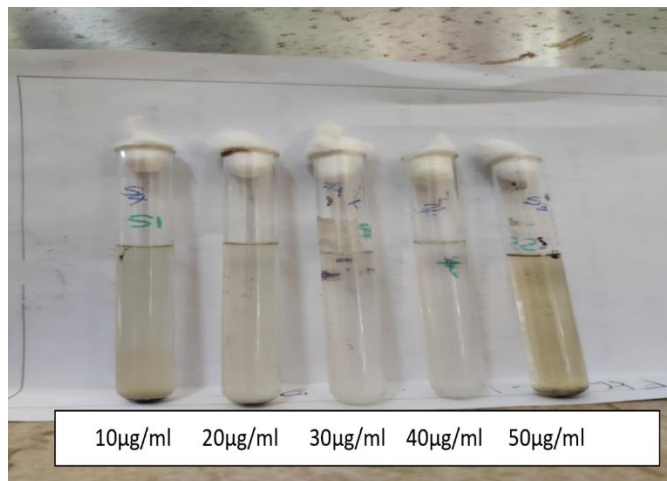


Figure 10: Turbidity of broth decreases as the increase in the concentration of AgNPs

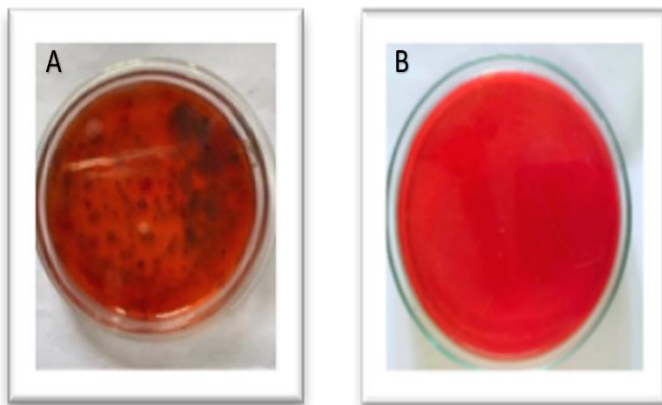


Figure 11: (A) Control plate and (B) Plate treated with AgNPs

Microtiter plate method

To evaluate the capacity of AgNPs to impede biofilm development, researchers employed crystal violet staining techniques. The reduction in color intensity clearly indicates the extent of biofilm inhibition. Treatment with higher concentrations of AgNPs, ranging from 50 to 200 µg/mL, resulted in increased anti-biofilm formation in the tested bacterial strains (Figure 12). The observed biofilm inhibition specifically targeted *P.aeruginosa*. The results reinforce the understanding of AgNPs biological impact, as observed in previous studies.³⁴

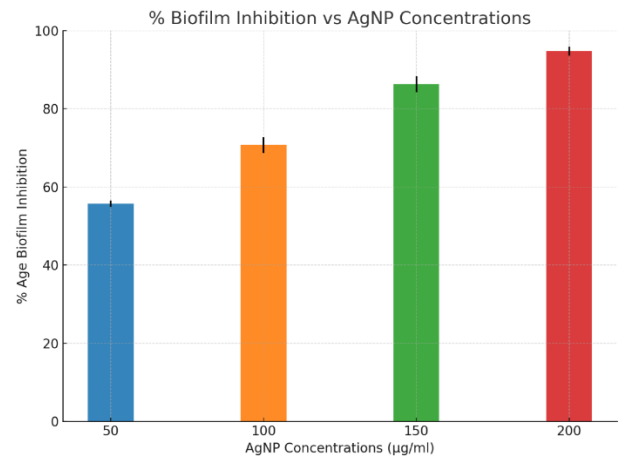


Figure 12: Reduction in violet color intensity due to increase in concentration of AgNPs

Conclusion

In conclusion, the research demonstrated the AgNPs were effectively biosynthesized through a simple, safe process utilizing the extracts of three leaves - *Raphanus sativus*, *Ipomoea batatas*, and *Ananas comosus*. The leaf extracts function as reducing agents for nanoparticle synthesis. Characterization of silver nanoparticles were performed using various analytical techniques like SEM showed the rod shaped and TEM revealed the spherical morphology, UV-Vis spectroscopy, FTIR, XRD, and DLS confirmed the presence of AgNPs. These nanoparticles demonstrated a maximum inhibitory zone against *Pseudomonas aeruginosa* at 100µg/ml and exhibited a minimum concentration to inhibit bacterial growth at 50µg/dl. At 200µg/ml, AgNPs displayed antibiofilm activity against *P.aeruginosa*. These results indicate that green-synthesized AgNPs from the aqueous extract of the three-leaf combination (*Raphanus sativus*, *Ipomoea batatas*, and *Ananas comosus*) may be effectively utilized to control biofilm formation against *Pseudomonas aeruginosa*. Moreover, in-depth investigations into the molecular mechanisms behind the antibacterial and antibiofilm activities could offer valuable insights into the precise interactions between the nanoparticles and microbial cells, as well as potential resistance pathways. The biocompatibility and toxicity of these nanoparticles in vivo must also be thoroughly evaluated to ensure their safety for clinical use.

Conflict of interest

The authors declare that they have no conflict of interests.

Author's declaration

The authors hereby declare that the work presented in this article is original and that any liability for claims relating to the content of this article will be borne by them.

Acknowledgements

The authors sincerely thank Dr. N. Ravichandran, Assistant Professor at SRC, SASTRA University, Kumbakonam, for his valuable assistance in identifying the plant specimens and assigning the voucher specimen numbers: *Raphanus sativus* (CARISM00203), *Ipomoea batatas* (CARISM00204), and *Ananas comosus* (CARISM00205).

References

- Lih HT, Airemwen CO, Halilu EM. Phytochemical Studies and Evaluation of Silver Nanoparticles Synthesized from *Solanum elaeagnifolium* Leaves Extract for Antioxidant and Antibacterial Activities. Trop J Nat Prod Res. 2024; 8(2):6440–6445
- Bijang CM, Joris SN, Hasanela N, Gaspersz N, Waremra A. Phytosynthesis and Antibacterial Activity of Silver Nanoparticles of Aqueous Extracts of Gandaria (*Bouea macrophylla* G.) Leaves and Stem Bark. Trop J Nat Prod Res. 2024;8(11):9315-9321.
- Adesipe-Olugbemi IT, Omotayo O. Biogenic synthesis and primary characterization of silver nanoparticles using aqueous extract of unripe banana peel; in vitro assessment on antioxidant and antibacterial properties. Trop J Nat Prod Res. 2020;4(11):990-994.
- Majumdar M, Dubey A, Goswami R, Misra TK, Roy DN. In vitro and in silico studies on the structural and biochemical insight of anti-biofilm activity of andrograpanin from *Andrographis paniculata* against *Pseudomonas aeruginosa*. World J Microbiol Biotechnol. 2020;36:1-18.
- Rather MA, Mandal M. Attenuation of biofilm and quorum sensing regulated virulence factors of an opportunistic pathogen *Pseudomonas aeruginosa* by phytofabricated silver nanoparticles. Microb Pathog. 2023;185:106433.
- Giri AK, Jena B, Biswal B, Pradhan AK, Arakha M, Acharya S, Acharya L. Green synthesis and characterization of silver nanoparticles using *Eugenia roxburghii* DC. extract and activity against biofilm-producing bacteria. Sci Rep. 2022;12(1):8383.
- Soliman NA, EL-Gaafary NM, Shalaby AA, Hussein OM, Taha NM. Physiological and Histopathological Effects of Two Seed Extracts (*Phoenix dactylifera* and *Raphanus sativus*) and L-Carnitine Drug on Semen Quality and Testicular Sexual Hormonal Changes in Adult Male Rabbits. Trop J Nat Prod Res. 2021;5(10):1709-1715.
- Kusumo GG, Dipahayu D. The Effect of Nano Extract Formulation on Antioxidant Activity of 70% Ethanolic Extract of Purple Sweet Potato's Leaves (*Ipomoea batatas* L.) Antin-3 Variety. J Pharm Sci. 2022;7(1):43-47.
- Mayasari D, Islami D, Oktariani E, Wulandari P. Phytochemical, Antioxidant and Antibacterial Evaluations of *Ipomoea batatas* L. from Riau, Sumatera Island, Indonesia. Trop J Nat Prod Res. 2023;7(1):2157-2162. doi:10.26538/tjnpr/v7i1.11.
- Trinanda R, Sundaryono A, Handayani D. Pembuatan Nanopartikel-Perak Ekstrak Daun Ubi Jalar Orange (*Ipomoea Batatas* L.) Dengan Metode Bioreduksi Dan Uji Aktivitas Terhadap Jumlah Trombosit Mus musculus. Alotrop. 2019;3(1).
- Kumar R, Gokul S, Ran F, Sambasivam S, Alrashidi KA, Thangappan R. Green synthesis of g-C₃N₄ decorated with SnO₂ nanocomposites using a novel *Ananas comosus* crown extract for boosted performance of asymmetric supercapacitors. J Energy Storage. 2024;98:113231.
- Alnaddaf LM, Almuhammady AK, Salem KF, Alloosh MT, Saleh MM, Al-Khayri JM. Green synthesis of nanoparticles using different plant extracts and their characterizations. silver nanoparticles using *Azadirachta indica* bark extract and its antibacterial application. J Agric Food Res. 2024;16:101088.
- Ahmed S, Ahmad M, Swami BL, Ikram S. Green synthesis of silver nanoparticles using *Azadirachta indica* aqueous leaf extract. J Radiat Res Appl Sci. 2016;9(1):1-7.
- Katta VKM, Dubey RS. Green synthesis of silver nanoparticles using *Tagetes erecta* plant and investigation of Nanobiotechnology: Mitigation of Abiotic Stress in Plants. 2021:165-199.
- Kumari SC, Selvakumar V, Padma PN, Anuradha K. Optimization studies on green synthesis of silver nanoparticles from different plant extracts using Taguchi design. Indian J Sci Technol. 2021;14:2888-2898.
- Alnaddaf LM, Almuhammady AK, Salem KF, Alloosh MT, Saleh MM, Al-Khayri JM. Green synthesis of nanoparticles using different plant extracts and their characterizations. Nanobiotechnology: Mitigation of Abiotic Stress in Plants. 2021:165-99.
- Maduraimuthu V, Ranishree JK, Gopalakrishnan RM, Ayyadurai B, Raja R, Heese K. Antioxidant activities of photoinduced phylogenetic silver nanoparticles and their potential applications. Antioxidants. 2023;12(6):1298.
- Jyoti K, Baunthiyal M, Singh A. Characterization of silver nanoparticles synthesized using *Urtica dioica* Linn. leaves and their synergistic effects with antibiotics. J Radiat Res Appl Sci. 2016;9(3):217-227.
- Vallinayagam S, Rajendran K, Sekar V. Green synthesis and characterization of silver nanoparticles using Naringi crenulate leaf extract: key challenges for anticancer activities. J Mol Struct. 2021;1243:130829
- Zulfiqar Z, Khan RRM, Summer M, Saeed Z, Pervaiz M, Rasheed S, Ishaq S. Plant-mediated green synthesis of silver nanoparticles: synthesis, characterization, biological applications, and toxicological considerations: a review. Biocatal Agric Biotechnol. 2024;103121.
- Mohanta YK, Biswas K, Jena SK, Abd_Allah EF, Mohanta TK. Anti-biofilm and antibacterial activities of silver nanoparticles synthesized by the reducing activity of phytoconstituents present in Indian medicinal plants. Front Microbiol. 2020;11:1143.
- Shaikh S, Nazam N, Rizvi SMD, Ahmad K, Baig MH, Lee EJ, Choi I. Mechanistic insights into the antimicrobial actions of metallic nanoparticles and their implications for multidrug resistance. Int J Mol Sci. 2019;20(10):2468.
- Maiti S, Krishnan D, Barman G, Ghosh SK, Laha JK. Antimicrobial activities of silver nanoparticles synthesized from *Lycopersicon esculentum* extract. J Anal Sci Technol. 2014;5:1-7.
- Kalishwaralal K, BarathManiKanth S, Pandian SRK, Deepak V, Gurunathan S. Silver nanoparticles impede the biofilm formation by *Pseudomonas aeruginosa* and *Staphylococcus epidermidis*. Colloids Surf B Biointerfaces. 2010;79(2):340-344.
- Zaki NH, Husain Z. Enhanced antibacterial and anti-biofilm activities of biosynthesized silver nanoparticles against pathogenic bacteria. J Genet Environ Res Conserv. 2016;4(2):197-203.
- Tailor G, Yadav BL, Chaudhary J, Joshi M, Suvalka C. Green synthesis of silver nanoparticles using *Ocimum canum* and their anti-bacterial activity. Biochem Biophys Rep. 2020;24:100848.
- Verduzco-Chavira K, Vallejo-Cardona AA, González-Garibay AS, Torres-González OR, Sánchez-Hernández IM, Flores-Fernández JM, Padilla-Camberos E. Antibacterial and Antibiofilm Activity of Chemically and Biologically Synthesized Silver Nanoparticles. Antibiotics. 2023;12(7):1084.
- Singhal M, Loveleen L, Manchanda R, Syed A, Bahkali AH, Wong LS, Gupta N. Design, synthesis and optimization of their structural, optical, chemical and morphological properties. Mater Today Proc. 2021;45:794-798.
- Wypij M, Jędrzejewski T, Trzcińska-Wencel J, Ostrowski M, Rai M, Golińska P. Green synthesized silver nanoparticles: antibacterial and anticancer activities, biocompatibility, and analyses of surface-attached proteins. Front Microbiol. 2021;12:632505.

30. Aktepe N, Erbay N, Baran A, Firat Baran M, Keskin C. Synthesis, characterization, and evaluation of the antimicrobial activities of silver nanoparticles from *Cyclotrichium origanifolium* L. Int J Agric Environ Food Sci. 2022;6(3):426-434.
31. Ashraf H, Anjum T, Riaz S, Naseem S. Microwave-assisted green synthesis and characterization of silver nanoparticles using *Melia azedarach* for the management of Fusarium wilt in tomato. Front Microbiol. 2020;11:238.
32. Barabadi, H., Mojab, F., Vahidi, H., Marashi, B., Talank, N., Hosseini, O., & Saravanan, M. (2021). Green synthesis, characterization, antibacterial and biofilm inhibitory activity of silver nanoparticles compared to commercial silver nanoparticles. Inorganic Chemistry Communications, 129, 108647.
33. Loo, Y. Y., Rukayadi, Y., Nor-Khaizura, M. A. R., Kuan, C. H., Chieng, B. W., Nishibuchi, M., & Radu, S. (2018). In vitro antimicrobial activity of green synthesized silver nanoparticles against selected gram-negative foodborne pathogens. Frontiers in microbiology, 9, 1555.
34. Singhal, M., Chatterjee, S., Kumar, A., Syed, A., Bahkali, A. H., Gupta, N., & Nimesh, S. (2021). Exploring the antibacterial and antibiofilm efficacy of silver nanoparticles biosynthesized using *Punica granatum* leaves. Molecules, 26(19), 5762.